Simplified dynamics of a moored submerged buoy

J. Orszaghova[1], **H. Wolgamot**[1], **R. Eatock Taylor**[2], **S. Draper**[1], **A. Rafiee**[3], **P. H. Taylor**[2]
[1] Faculty of Engineering, Computing and Mathematics, University of Western Australia, Crawley, WA 6009, Australia. jana.orszaghova@uwa.edu.au
[2] Department of Engineering Science, University of Oxford, OX1 3PJ, UK.
[3] Carnegie Wave Energy Limited, Fremantle, WA 6160, Australia.

1 INTRODUCTION

This investigation is inspired by results from model scale laboratory tests carried out by Carnegie Wave Energy. The device tested is a 1:20 model of CETO 6, which is a buoyant submerged taut-moored point absorber WEC (wave energy converter). The device resembles a rather flat cylinder (axis vertical).

Testing was primarily in irregular waves, though a smaller selection of regular wave tests was carried out. Due to the axi-symmetry of the device, one might expect that the response would be confined to the (x, z) plane, i.e. the surge, heave and pitch motions of CETO. However, in a number of tests, significant sway and roll motions were measured. Additionally, it was noted that the horizontal plane responses of the device were not always coincident with the driving wave frequency/frequencies.

Such observations are characteristic of instability, a topic investigated in various contexts in the literature (e.g. Paulling and Rosenberg, 1959; Koo et al., 2004). For this submerged body we have developed a simple model, with linear hydrodynamics and weakly non-linear geometry, with the aim of predicting the occurrence of Mathieu-type instability in sway, and this matches the experimentally observed buoy behaviour quite well.

2 MODEL DERIVATION

The buoyant WEC is attached to the bottom of the tank via a tether, which is pre-tensioned to keep the device submerged. The tether (together with a winch and a pulley system) also acts as a PTO mechanism. When excited by incoming waves, the device can respond in 6 degrees of freedom. Thus the forces acting on the WEC are buoyancy minus self-weight, hydrodynamic forces and PTO forces. Fig. 1 shows a diagram of the WEC under consideration, assuming a 2D setup.

The net **buoyancy force** $F_B = \rho V g - mg$ acts vertically upwards, where ρ is the fluid density, V and m are the buoy volume and mass, and g is the magnitude of the gravitational acceleration.

The **PTO forces** (also referred to as tension forces) F_{PTO} act along the tether. For these experiments the PTO implemented is composed of a pre-tension force, a linear spring restoring force and a linear damping force, such that

$$F_{PTO} = C + K\Delta L + B\Delta\dot{L} \tag{1}$$

where C is the pre-tension term (equal to F_B), K is the linear spring coefficient and B is the linear damping coefficient. ΔL is referred to as PTO extension and denotes the change in tether length (which corresponds to piston stroke in the full scale hydraulic pump PTO). $\Delta\dot{L}$ is referred to as PTO velocity, and represents the rate of change of the tether length. PTO extension and velocity can be expressed in terms of Cartesian buoy motion variables as $\Delta L = \sqrt{(L+Z)^2 + X^2 + Y^2} - L$ and $\Delta\dot{L} = \frac{X\dot{X}+Y\dot{Y}+(L+Z)\dot{Z}}{\sqrt{(L+Z)^2+X^2+Y^2}}$, where L is the initial/static rope length; X, Y and Z are surge, sway and heave; and $\dot{X}$, $\dot{Y}$ and $\dot{Z}$ are the respective velocities. Note that for simplicity buoy rotations have been excluded in the above.

We decompose the tension force F_{PTO} into its horizontal and vertical components, using Fig. 1. Approximate expressions for each F_{PTO} component are also derived using multi-variable Taylor series, such that terms up to second order have been retained. Hence

$$F_{PTOx} = F_{PTO}\frac{X}{\sqrt{(L+Z)^2 + X^2 + Y^2}} \approx \frac{C}{L}X + \Big(\frac{K}{L} - \frac{C}{L^2}\Big)XZ + \frac{B}{L}X\dot{Z} + ... \tag{2}$$

$$F_{PTOz} = F_{PTO}\frac{Z+L}{\sqrt{(L+Z)^2+X^2+Y^2}} \approx C + KZ + B\dot{Z} + \frac{1}{2}\left(\frac{K}{L} - \frac{C}{L^2}\right)(X^2+Y^2) + \frac{B}{L}(X\dot{X}+Y\dot{Y}) + \ldots \quad (3)$$

where the x- and y-directions are identical.

Excluding the buoy rotations, simplified equations of motion are given by

$$m_x\ddot{X} = -F_{PTOx} + F_{Wx}, \qquad m_x\ddot{Y} = -F_{PTOy}, \qquad m_z\ddot{Z} = -F_{PTOz} + F_{Wz} + F_B, \quad (4)$$

where $m_x = m + m_{11}$ and $m_z = m + m_{33}$, with m_{11} and m_{33} denoting the added mass in surge/sway and heave respectively. The F_W terms denote (the remainder of) the hydrodynamic forces. As we are interested in stability, we consider only homogeneous forms of the governing equations, at various orders of approximation. We thus neglect wave exciting force entirely, and, even though it would ultimately appear on the left-hand-side of the governing equations, radiation damping.

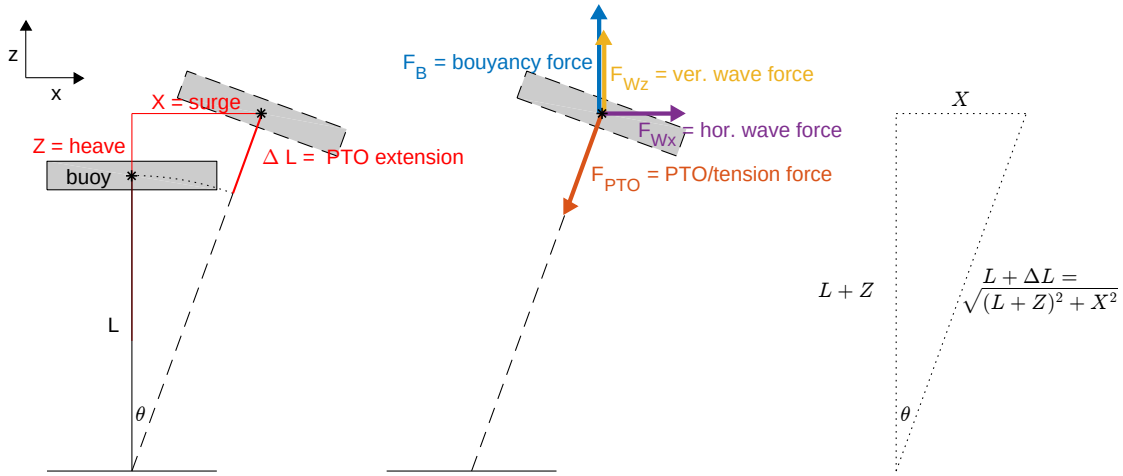

Fig. 1: Schematic diagram. For simplicity, only heave and surge shown.

3 LINEARISED MODEL

The governing homogeneous equations can be linearised, by retaining only first order terms from the Taylor expansions, as follows.

$$\ddot{X} + \frac{C}{m_x L}X = 0 \qquad \ddot{Z} + \frac{K}{m_z}Z + \frac{B}{m_z}\dot{Z} = 0 \quad (5)$$

To first order the equations are uncoupled. The restoring force in the horizontal directions is due to buoyancy/pre-tension. The vertical equation contains a linear damping term, whereas the horizontal motions are un-damped. The natural un-damped angular frequency in surge/sway, and the natural damped angular frequency in heave are given by

$$\omega_{nx} = \sqrt{\frac{C}{m_x L}} \qquad \omega_{dz} = \sqrt{\frac{K}{m_z} - \left(\frac{B}{2m_z}\right)^2} \quad (6)$$

Using added mass values from linear potential flow theory we compute the natural frequencies in surge and heave, and use the former to non-dimensionalise the frequency axis in Fig. 2, which shows the experimental motion spectra from an irregular waves run, as well as the input wave spectrum. The plots suggest that the computed values are reasonably accurate.

Clearly the simplified governing equations, given by Equation (5), with sinusoidal incident wave forcing, cannot capture non-linear phenomena such as response period doubling.

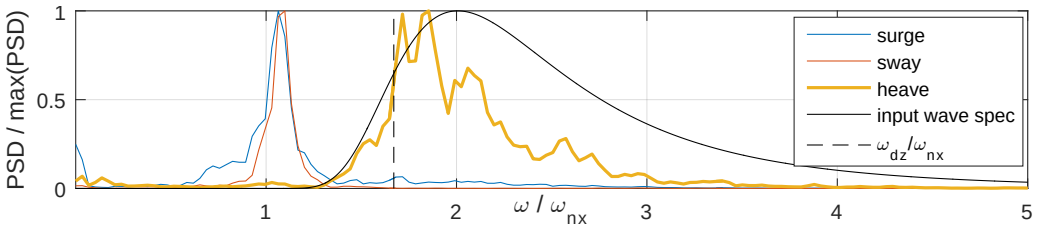

Fig. 2: Wave and response spectra from an irregular wave run.

4 SECOND ORDER MODEL

Retaining terms of up to second order, another set of approximate governing equations can be derived.

$$\ddot{X} + \Big(\frac{C}{m_x L} + \Big(\frac{K}{m_x} - \frac{C}{m_x L}\Big)\frac{Z}{L} + \frac{B}{m_x}\frac{\dot{Z}}{L}\Big)X = 0 \tag{7}$$

$$\ddot{Z} + \frac{K}{m_z}Z + \frac{B}{m_z}\dot{Z} + \Big(\frac{K}{m_z} - \frac{C}{m_z L}\Big)\Big(\frac{X^2+Y^2}{2L}\Big) + \frac{B}{m_z}\Big(\frac{X\dot{X}+Y\dot{Y}}{L}\Big) = 0 \tag{8}$$

Note that the governing equations are now rather complicated and are coupled again. Here we are concerned with determining stability in the horizontal translations. The sway (or surge) governing equation contains product terms YZ and $Y\dot{Z}$. We empirically observe the experimental heave response in regular waves to be approximately sinusoidal (at the wave frequency ω), as Equation (5) might suggest. The governing equation for sway may therefore be recast in such a way that it represents an un-damped mass-spring system, with a constant and a time-varying spring coefficient.

$$\ddot{Y} + \Big(\omega_{nx}^2 + \alpha\cos(\omega t + \phi)\Big)Y = 0 \tag{9}$$

This is the classical (undamped) Mathieu equation, and α and ϕ represent the amplitude and the phase of the time-varying spring coefficient. Without loss of generality the phase can be chosen to be 0, and the amplitude expression, in terms of heave amplitude Z_a, is given below.

$$\alpha = \frac{Z_a}{m_x L}\sqrt{\Big(K - \frac{C}{L}\Big)^2 + B^2\omega^2} \tag{10}$$

We reformulate the equation using $\omega t = 2\tau$, such that

$$\ddot{Y} + \Big(4\Big(\frac{\omega_{nx}}{\omega}\Big)^2 + 4\frac{\alpha}{\omega^2}\cos(2\tau)\Big)Y = 0 \tag{11}$$

where the derivatives are now with respect to τ. Here we adopt the harmonic balance method to find the stability curves (e.g. Moideen and Falzarano, 2010). This leads to a non-linear algebraic equation in $\delta = 4(\frac{w_{nx}}{w})^2$ and $\epsilon = 2\frac{\alpha}{\omega^2}$, which can be solved numerically for a given range of one of the variables.

The calculated stability diagram is presented in Fig. 3a. Regions above the red curves correspond to unstable solutions, whereas regions below the curves represent stable solutions.

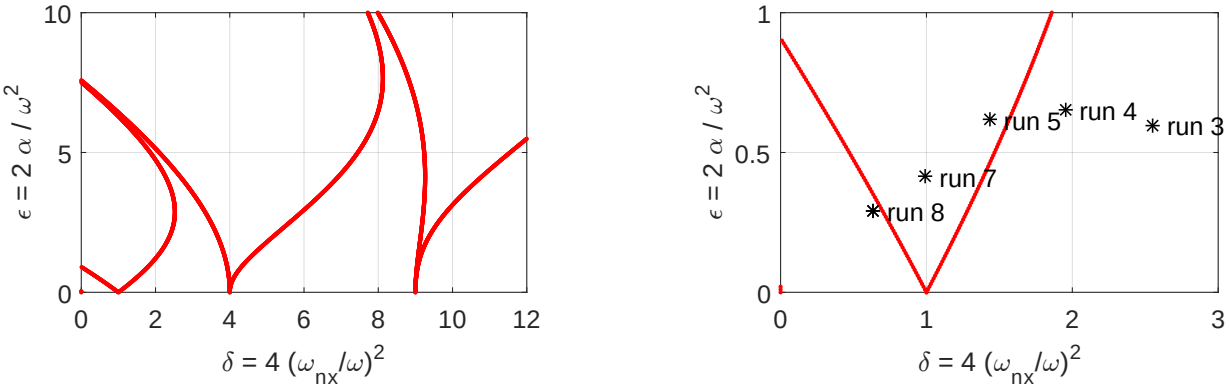

(a) Stability diagram. **(b) Five regular waves experiments.**

Fig. 3: Stability diagram with five regular waves experiments.

We are interested in whether this model is useful in predicting the occurrence of instability in regular wave experiments. Dots representing the five regular wave experiments conducted are shown in (δ,ϵ)-space on the zoomed-in diagram in Fig. 3b. Rather than solving the coupled equations to calculate α, and hence ϵ, we use the measured heave amplitude from the experiment. It is seen that points exist in the stable and unstable regions.

Motion timeseries from the four (out of five) regular waves experiments considered are shown in Fig. 4a to 4d. Note that the equivalent plot from Run 3 is omitted for brevity. It does not exhibit sway instability, and the motion timeseries are very similar to those from Run 4. It is apparent (particularly from the sway timeseries) that the stability predictions are correct for Runs 3-7, and the phenomenon of subharmonic (period doubling) response is clearly seen in Runs 5 and 7. Run 8, which appears on the stability boundary, is more difficult to comment on.

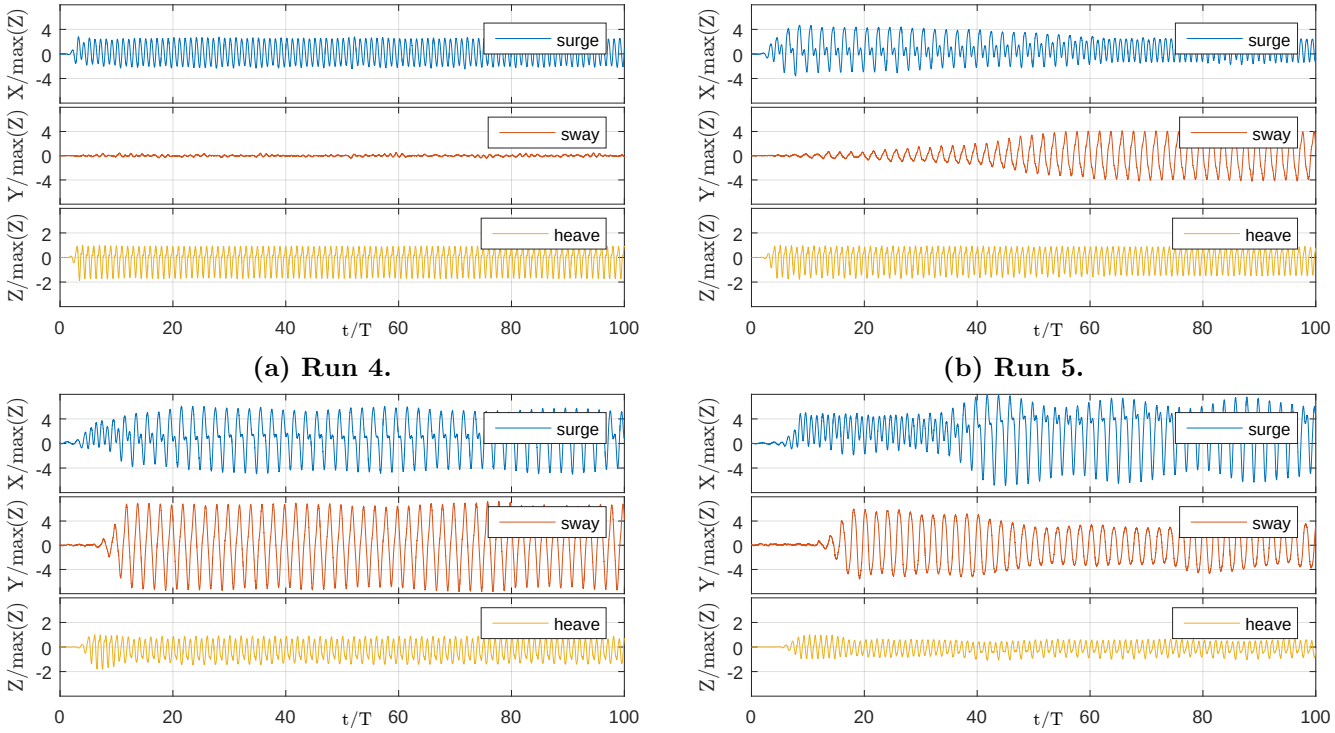

(a) Run 4. **(b) Run 5.**

(c) Run 7. **(d) Run 8.**

Fig. 4: Measured buoy motion from regular waves experiments.

Further experimental data is being obtained to provide additional tests of the theory, and will be presented at the Workshop. Numerous additions to this investigation are intended, including the addition of radiation damping, consideration of instability in irregular waves and additional sources of instability including position-varying exciting force (Eatock Taylor and Knoop, 1981).

This research was supported under Australian Research Council's Linkage Project scheme (LP150100598). Provision of the experimental data from Carnegie Wave Energy is gratefully acknowledged.

REFERENCES

R Eatock Taylor and J Knoop. Dynamic instability of a freely floating platform in waves. In *Design for Dynamic Loading The Use of Model Analysis*, pages 57–62, 1981.

BJ Koo, MH Kim, and RE Randall. Mathieu instability of a spar platform with mooring and risers. *Ocean Engineering*, 31(17):2175–2208, 2004.

H Moideen and J Falzarano. A critical assessment of ship parametric roll analysis. In *Proceedings of the 11th International Ship Stability Workshop (ISSW)*, pages 272–279, 2010.

JR Paulling and RM Rosenberg. On unstable ship motions resulting from nonlinear coupling. *Journal of Ship Research*, 3(1):36–46, 1959.